Bulletin of the Seismological Society of America, Vol. 87, No. 6, pp. 1463–1472, December 1997

Seismological Studies at Parkfield V: Characteristic Microearthquake Sequences as Fault-Zone Drilling Targets

by R. M. Nadeau and T. V. McEvilly

Abstract Studies at very high resolution of microearthquakes at Parkfield, California, since 1987 reveal a systematic organization in space and time, dominated by clustering of nearly identical, regularly occurring microearthquakes (characteristic events) on 10 to 20-m-wide patches within the fault zone. More than half of the 4000+ events in our 1987 to 1996 catalog exhibit this trait. In general, recurrence intervals (0.5 to 2 yr) scale with the magnitude of the repeating events for the on-scale range (*Mw* 0.2 to 1.3) in this study. The similar waveforms, superimposed locations, quasi-periodic recurrence, and uniform size of these characteristic events permit relative hypocenter location accuracy of meters and predictable occurrence times within windows of a few months. Clustered characteristic events occur at depths as shallow as about 3 km, and these are feasible targets for deep scientific drilling and observation at the focus of a subsequent small earthquake within an active plate-boundary fault zone. At Parkfield, the achievable location accuracy to which a hypocenter can be specified as well as the predictability of its occurrence time appear to be uniquely favorable for *in situ* fault-zone measurements.

Introduction and Motivation

Previous seismological studies at Parkfield, California, have revealed a process in ongoing seismicity that is characterized by highly organized and stable clustering of nearly identical, regularly occurring microearthquakes, and this type of activity is representative of more than half of the earthquakes recorded there (Nadeau *et al.,* 1994, 1995). Repeating similar earthquakes of this type are called "characteristic," and they have been used to model recurring large earthquakes (e.g., Schwartz and Coppersmith, 1984). Operation since 1987 of a network of 10 deeply buried (200 to 300 m) three-component high-sensitivity seismographs at Parkfield (HRSN, the High-Resolution Seismographic Network) has produced a sharpened definition of seismicity and fault-zone structure (see Fig. 1). The low-noise, low-attenuation, and reduced near-surface coda generation inherent in deep sensor emplacement allows for routine recording of three-component waveforms above background noise across a bandwidth of 125 Hz from earthquakes as small as $M = -0.5$ so that the 1987 to 1996 catalog contains more than 4000 events along the ~25-km segment of the San Andreas fault being monitored and presumed to be the nucleation zone for repeating M 6 earthquakes (Bakun and McEvilly, 1984). The network is part of the intensive instrumentation deployed in the Parkfield Prediction Experiment (Bakun and Lindh, 1985).

The very highly organized spatio-temporal structure exhibited in the earthquake process at Parkfield had not been identified in previous investigations, as we shall illustrate, because of limited resolution attained in the routine application of conventional hypocentral location methods to microearthquakes. The resulting relatively low spatial resolution arises because variance in the location estimate does not scale and improve with decreasing event size. In fact, variance worsens due to decreasing signal strength and consequent poorer event detection and arrival-time measurement. While conventionally derived hypocenters with location uncertainties of 1 to 2 km or more in the point of rupture initiation on the fault are considered to be high resolution for M 6 or larger earthquakes having source dimensions greater than 20 km, such uncertainties are inadequate in studies of spatial distributions for microearthquakes at the M 1 level that have source radii of 10 to 20 m (assuming a stress drop around 3 MPa).

In ongoing Parkfield research, we have been examining the resolution limits for relative and absolute hypocenter location estimates using the Parkfield HRSN data. Additionally, we are characterizing the degree of stability in the recurrence intervals for many of the sequences of repeating events there. Coincident with this work, the idea of drilling deeply into the San Andreas fault at Parkfield was being developed (Hickman *et al.,* 1994), with shallow clustered hypocenters as potential targets. Clearly, the accuracy to which we can specify a hypocenter and its time of occurrence are critical considerations in devising a drilling plan if

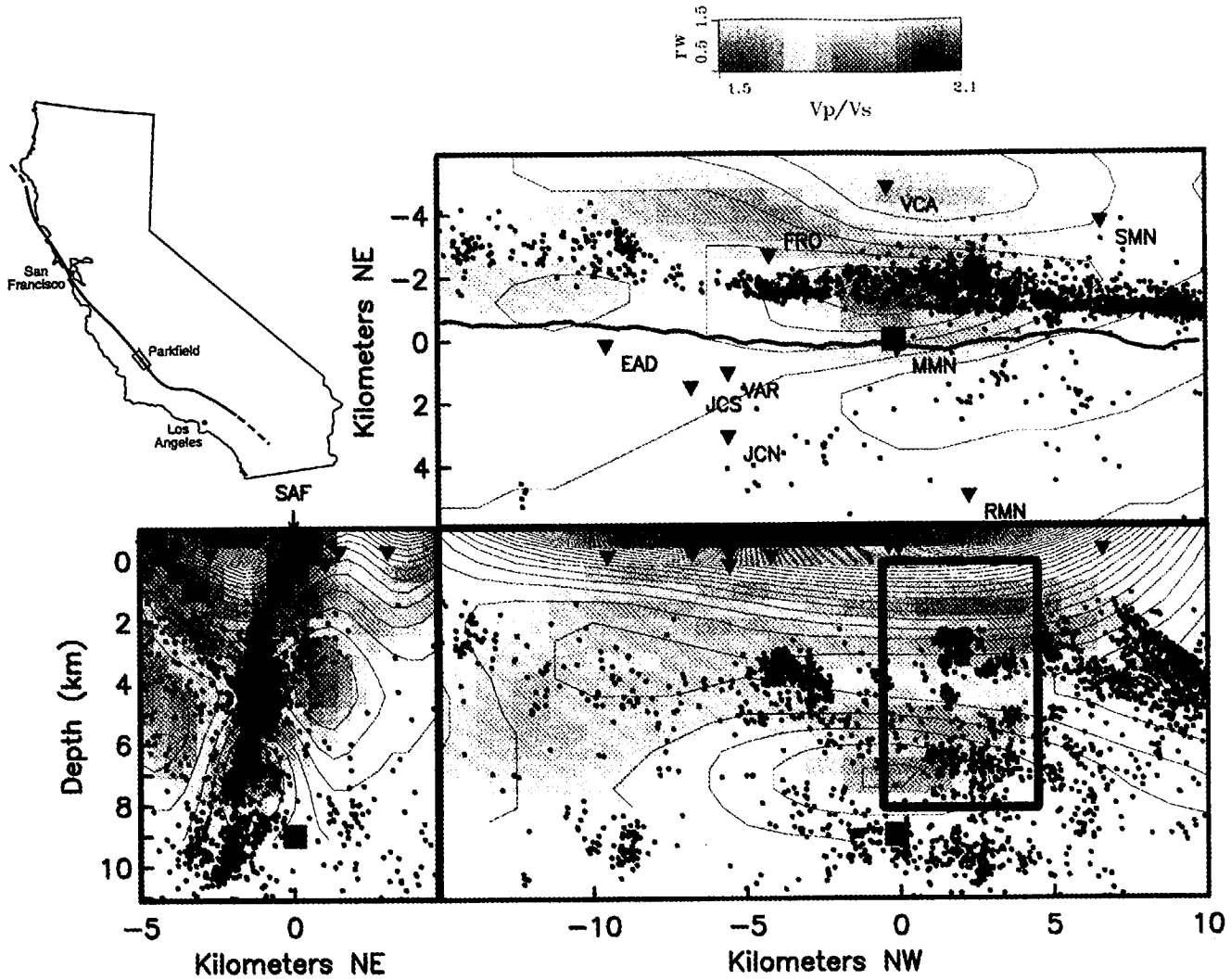

Figure 1. Study area at Parkfield, California, with plan and cross-section displays of projected 1987 to 1996 hypocenters (black dots) and the estimated *Vp/Vs* seismic velocity ratio along the fault zone. The plan view (upper frame) shows *Vp/Vs* at 6.8 km depth. The lower frames are sections across (*left*) and along the fault zone, referenced to sea level. Triangles are stations, red dots are the microearthquake clusters discussed in the text, and the square symbol is the hypocenter of the 1966 magnitude 6 event at Parkfield. The black line shows the surface position of the San Andreas fault. The box delineates the part of the fault zone considered for deep drilling to one of the clusters and matches in dimensions the panels in Figure 4.

a scientific goal is real-time *in situ* measurement of the rupture process. To explore these issues in this article, we analyze the location resolution achievable for a specific control group of 60 shallow microearthquakes within drilling range at Parkfield and then consider the recurrence stability for repeating sequences within this group.

Comparing Hypocenter Catalogs

We compare a set of hypocenters in the common catalogs that cover Parkfield seismicity to demonstrate that substantial improvement can be achieved over conventionally estimated locations for clusters of similar events. The comparison was made for a control group of 60 microearthquakes at the proposed Parkfield drilling site (Fig. 1) as reported in five different earthquake catalogs that include the region:

C1. The NCSN catalog based on observations of *P*-wave arrival times from the USGS network with station corrections.
C2. The Duke University catalog that uses automatically picked *P*- and *S*-wave arrivals and a one-dimensional velocity model developed using events recorded since 1988 on the HRSN network only.
C3. The Berkeley catalog of events recorded since 1987 on

the HRSN and located with rms residuals <50 msec (typically around 20 msec). Here, hypocenters were determined using routinely hand-picked *P*- and *S*-wave arrivals (generally 10 to 12 per event) and three-dimensional *P* and *S* velocity models for Parkfield developed using a joint inversion of CALNET *P* and HRSN *P* and *S* arrival times (Michelini and McEvilly, 1991).

C4. The Berkeley relative location catalog that uses the same data and velocity models as C3, and a relative event location method based on Fremont and Malone (1987). Here, differential times between a consistent station set of *P* and *S* phases—the same set of phases (generally 10 to 12) for all events in a cluster—are determined for events in each cluster relative to a reference event for that cluster. This is done to nearest sample precision (+/−1 msec) using waveform cross-correlation (254- and 510-msec windows for *P* and *S* phases, respectively). Similarly, differential times are determined between neighboring cluster reference events. The differentials are then used to relocate the reference events relative to each other and to the centroid of their locations. The remaining events, within the clusters, are then relocated relative to their respective reference events resulting in the final multi-cluster constellation of catalog hypocenters.

C5. A Berkeley catalog that takes the methodology of C4 one step further by employing subsample precision techniques (Poupinet *et al.*, 1984) within cluster groups in an attempt to resolve location differences at the finest scale possible.

As expected, catalog completeness and resolution both improve with inclusion of the borehole network data and with more advanced methods for event identification and processing.

The control group of events grew from a set of 12 earthquakes with magnitudes 0.0 to 1.5 and depths 2 to 4 km that occurred since 1987 and that were initially identified using Northern California Seismic Network (NCSN) data as potential drilling targets (Ellsworth, 1996) in the "Kester group" of microearthquakes (named for the local landowner). In the HRSN data base, we found the 12 events to be members of seven distinct, nonoverlapping earthquake clusters that contained at least 60 earthquakes in total. There were likely more than 60 events in the Kester group of seven clusters during the period, some surely having been missed due to equipment outages or failure of the network to trigger on an event. Also, the 60 events and their seven clusters share the local fault zone with roughly twice as many events and clusters, so that the rate of seismicity in the potential drilling volume is in fact triple that discussed in this study.

We use the term "cluster" for the distinct groups of highly similar earthquakes whose waveforms exhibit cross-correlation coefficients >0.98 and whose locations, as a consequence, concentrate on small patches in the fault zone. Within some such clusters, we find adjacent subcluster groupings of events with very subtle waveform differences yet still satisfying the >0.98 correlation criterion. Clusters of highly similar microearthquakes are ubiquitous throughout the fault zone at Parkfield, where nearly two-thirds of the ongoing microseismicity occurs in some 300 of these small clusters (Nadeau *et al.*, 1995). Our identification of cluster and subcluster members is based primarily on the similarity of seismograms, initially characterized using cross-correlation (see Aster and Scott, 1993), with further discrimination based on visual inspection to identify subtle yet systematic patterns in the waveforms not discerned by the cross-correlations. We find this approach to be more effective for the broadband borehole data than selection methods based on event size, recurrence times, or locations—parameters that are ultimately derived from the original seismograms anyway.

We began our analysis of the 12 target events by searching C1 out to 25 km range from the Kester group for mislocated group members in that catalog and found eight additional events in the group of 60. C1 thus contains 20 of the 60 controls, consistent with a NCSN detection completeness around $Mw = 0.9$ at Parkfield. C2 contains 49 (C2 did not archive 5 of the 60 that occurred in 1987) and C3 through C5 list 59 of the 60 controls; these HRSN-based catalogs having missed an event during one of the Vibroseis monitoring sessions that temporarily take over the network (Karageorgi *et al.*, 1992). The 48 events added to the original 12 are unquestionably members of the same group of highly similar microearthquakes as shown in Figure 2. The NCSN seismogram in Figure 2 is from surface station PMM, only 224 m from HRSN station MMN (221 m deep). These seismograms illustrate the greatly enhanced signal quality and *S*-wave definition achieved in borehole installations. The 125-Hz bandwidth and low noise achievable in borehole installations yield the high resolution and sensitivity basic to this study. The sensitivity gain is evident in the $Mw \sim 0.7$ difference in completeness between the catalogs evident in Figure 3.

Spatial Organization and Location Bias

The control group of hypocenters from the various catalogs is presented in Figure 4. Color-coded symbols track the different computed positions of the individual cluster members through the catalogs as their organization evolves into the seven distinct clusters labeled K1 to K7 in the final C4 and C5 frame. The ultimate resolution in C5 is achieved by estimating relative arrival times of *P* and *S* waves to subsample precision (Poupinet *et al.*, 1984), improving the basic +/−1 msec nearest-sample timing (2 msec sampling rate) used in C4 to about 0.4 msec, further reducing the scatter among cluster members by 25%.

C4 and C5 both show tight groupings of hypocenters in steeply dipping patches for all clusters of the control group, as illustrated for K6 in Figure 5 at 100 × expanded scale

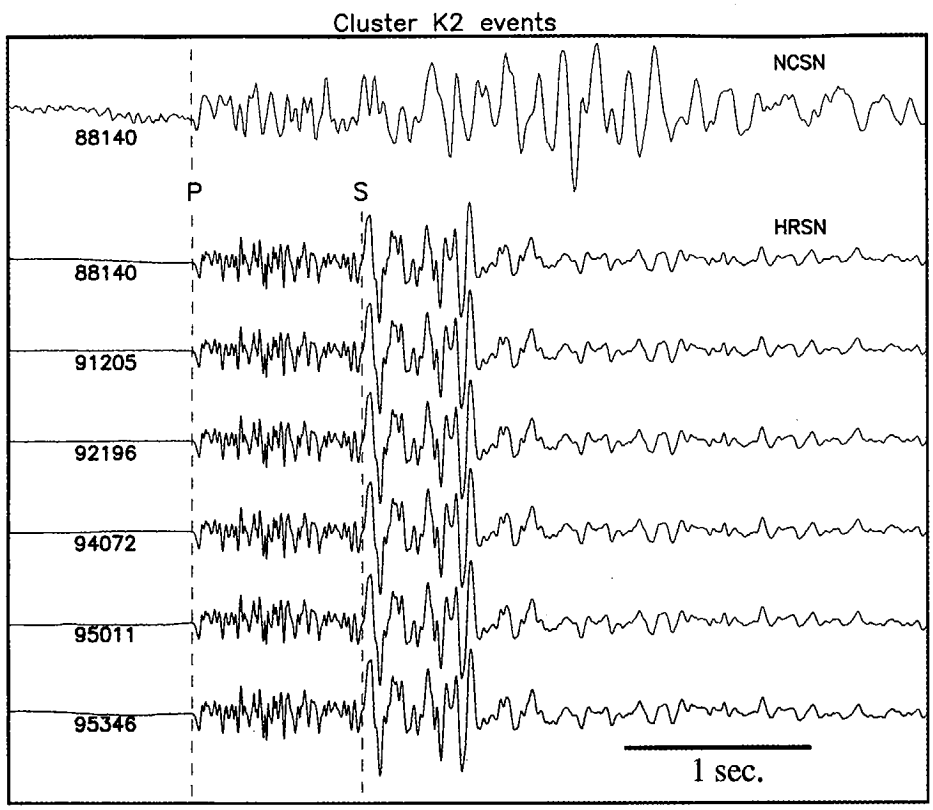

Figure 2. Vertical-component seismograms for one cluster (K2 in Fig. 4) in the Kester group from NCSN station PMM (*upper trace*) for the only event in catalog C1 for this cluster, and from HRSN borehole station MMN for that event and the other five similar events in cluster K2. PMM is located on the surface 224 m from the borehole in which station MMN is installed at 221 m depth. This striking waveform similarity was used to identify the other five K2 cluster members in the HRSN data base and is typical for all clusters at Parkfield. The high-frequency content and suppressed *S*-wave coda evident in the waveforms is characteristic of borehole recordings and illustrates their necessity in studies of fault-zone processes at very fine scale.

from Figure 4. At this resolution, cluster K6 is seen to be further organized into subclusters, a commonly observed occurrence of two or more event types differing slightly in waveforms and defining adjacent but nonoverlapping patches, and in some cases exhibiting distinct magnitudes or differing temporal behavior. This ultimate degree of subdivision places 58 of the 60 events in eight distinct clusters and subclusters of characteristic events on individual 10 to 20-m patches. In Figure 5, the small symbols are *Mw* 0.5 earthquakes of two types, and the large symbol is a single, as yet unrepeated, *Mw* 0.9 event in K6. Relative locations determined for the full Kester group, using the reference event in each cluster, define a flat, steeply dipping vertical strip about 1 km in width × 2 km in depth extent and aligned with the regional fault strike (dip 86.6 +/− 1.7° SW; strike 314.0 +/−4.4°; bottom two panels of Fig. 4).

The subsample timing analysis has been applied to signals having less high-frequency content than HRSN, with good results (e.g., Fremont and Malone, 1987). Generally, it appears that timing can be sharpened for similar "doublet" events to about one-fifth of the sampling interval. In Figure 6, application of the method to NCSN signals for cluster K4 of larger ($Mw \approx 1.3$) events in the Kester Group (W. L. Ellsworth, personal comm., 1996) is compared to HRSN results for K4. The differences are these: NCSN data are vertical component, bandwidth <20 Hz, *P* wave only; HRSN data are three-component, bandwidth ≈125 Hz, *P*- and *S*-wave arrivals used (a comparison of typical signals can be seen in Fig. 2). Analysis methods also differ somewhat in data selection and computational method, but degrees of relative location improvement are generally similar. Standard deviation of scatter about the K4 centroids are 16 and 5 m for NCSN and HRSN, respectively, the difference corresponding roughly to the square root of the bandwidth ratio, suggesting that for small events, unambiguous subcluster definition is likely impossible with the lower bandwidth data.

To assess resolution differences among the various catalogs, we assumed that the hypocenters within the eight characteristic sequences actually occurred at the centroids of the individual sequences, so that distances of the computed

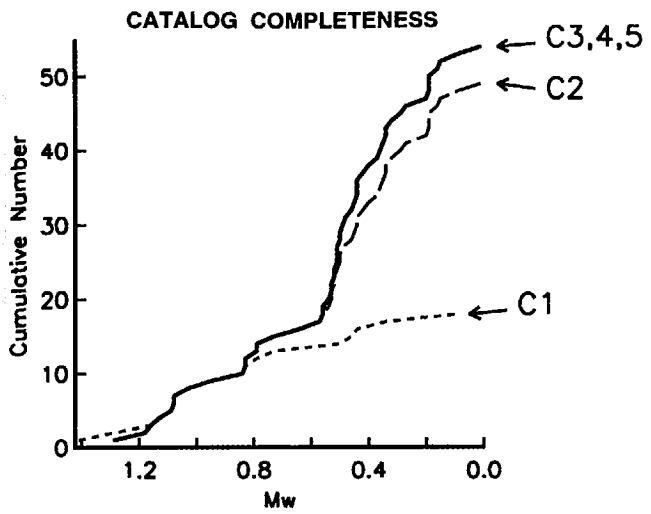

Figure 3. Completeness of the catalogs. Cumulative number of control-group events with decreasing magnitude for catalogs C1 through C5. The five events occurring in 1987 are omitted since catalog C2 begins in 1988. The sensitivity gain from the borehole instruments is evident in the *Mw* ~ 0.7 difference in completeness between the NCSN (C1) and HRSN (C2 through C5) catalogs and is consistent with a more generally observed completeness threshold for the NCSN of magnitude 0.9 at Parkfield.

locations from the eight centroids represent errors in hypocenter estimates. Under this assumption, the five catalogs differ in resolution by more than two orders of magnitude for the control group of earthquakes, as shown in Figure 7, where we plot the cumulative distributions of hypocenter-to-centroid distances for the five catalogs. We conclude from this analysis that high-quality data processed using subsample relative timing among highly similar waveforms can yield relative hypocenter location accuracy of about 5 m within similar event clusters and that individual subclusters can be easily distinguished when separated by as little as 10 m. Patch sizes of 5- to 10-m radius, based on the scatter of hypocenters, are seen for all clusters, and patch size appears to be independent of the magnitude of the member events (range *Mw* 0.2 to 1.3 in this study). Each hypocenter within a patch corresponds to a center of seismic moment release because cross spectra of entire *P* or *S* waveform pulses are used to estimate the time delays among the arrivals for each cluster. Our results cannot exclude exact colocation of the slip surfaces for the sequence members, given our timing accuracy, the seismic wave velocities at the source, possible temporal changes in propagation velocities, and the numerical estimation of the hypocenter.

It is important to keep in mind that, even with this precision in relative locations of clustered events, absolute location bias remains in the computed hypocenters due to errors in the velocity model, and a means to define and eliminate this bias must be addressed in developing a drilling scenario to penetrate a specific cluster in the Kester group.

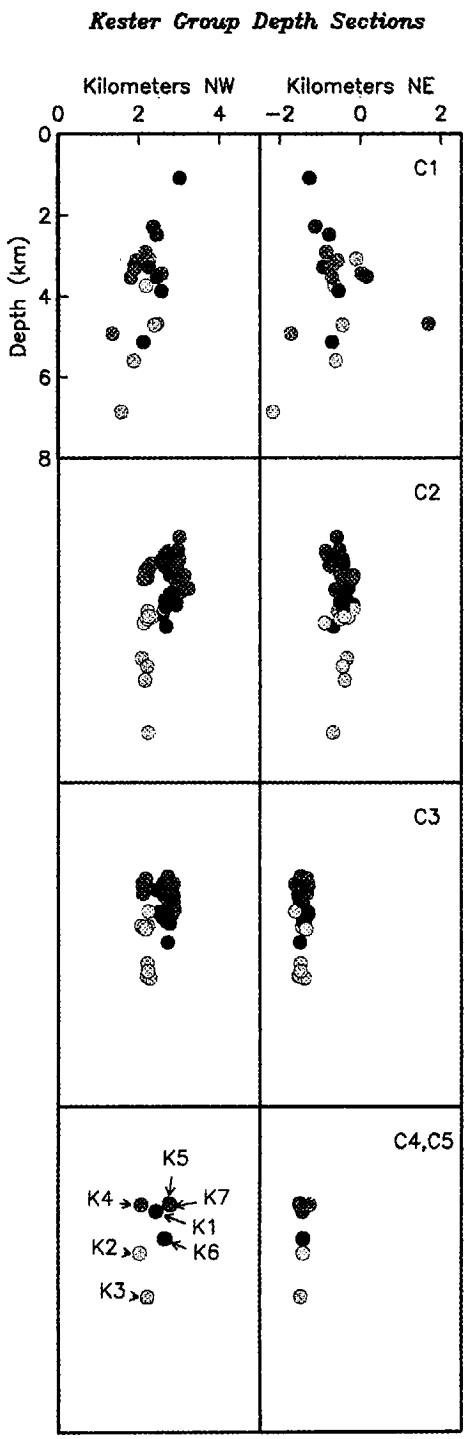

Figure 4. Hypocenter distributions. Comparison of catalog hypocenters in 5 × 8 km vertical sections oriented along and across the San Andreas fault. Color symbols define members of the seven distinct clusters that we label K1 to K7 in the final C4 and C5 frames. Locations within the individual clusters for catalogs C4 and C5 are indistinguishable at this scale. Note how the apparently diffuse seismicity in catalog (C1), typical of routine microearthquake monitoring results, is actually a steeply dipping planar feature containing several clusters of adjacent and colocated events. Depths are given below mean sea level.

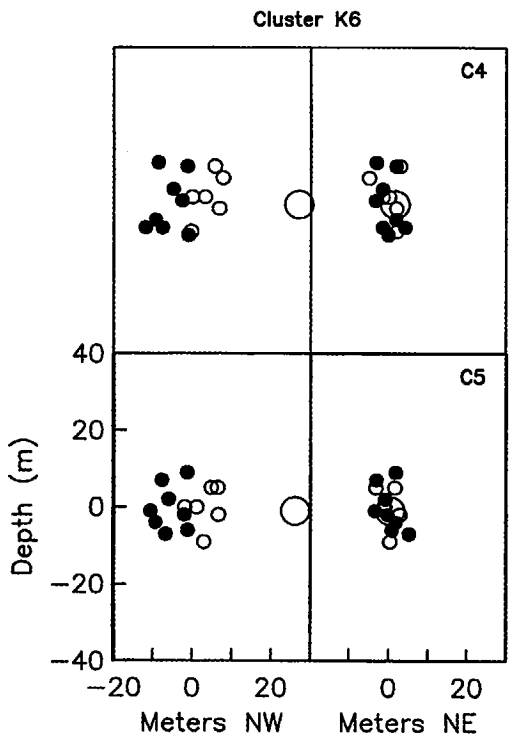

Figure 5. Maximum resolution. K6 events from Figure 4, at 100X expanded scale for C4 (nearest sample timing) and C5 (subsample timing), showing the distinct event types within a cluster (subclusters) that are visible at highest resolution. Small open and filled symbols are all magnitude 0.5 earthquakes, the large symbol is a magnitude 0.9 event. These patch shapes are typical of the 10- 20-m-diameter surfaces aligned with the regional fault strike that are found for many clusters.

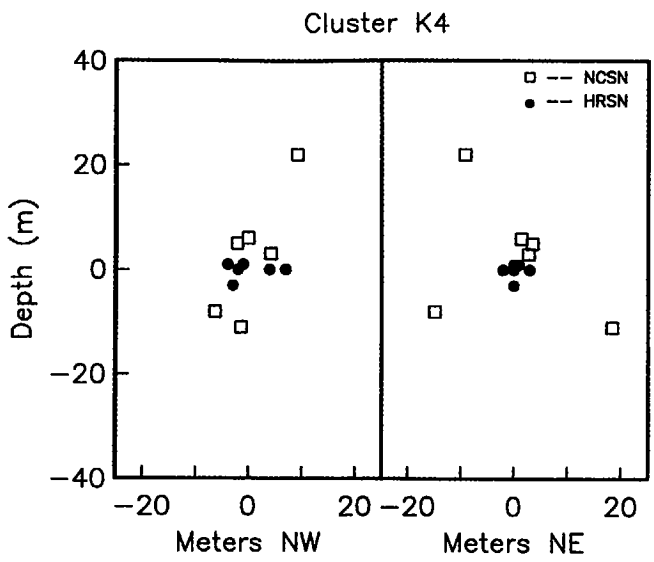

Figure 6. Relative locations using different data sets. Hypocenters for cluster K4 of larger ($Mw \approx 1.3$) events in the Kester Group from C5 at 100X expanded scale (filled circles), compared to relative locations (from Ellsworth, personal comm., 1996) computed using NCSN waveforms for the same K4 events (*open squares*). Cluster centroids are superposed for comparison. Typical signals of the two types can be seen in Figure 2. Standard deviations of hypocenter distances from the K4 centroids are 16 and 5 m for NCSN and HRSN, respectively. Discrimination of characteristic event types in small multiple-event-type clusters (e.g., K6) may not be possible using the lower bandwidth surface stations of the NCSN.

Bias in the absolute location of the target slip surface, due to the strong lateral velocity gradients across the fault zone, is likely to be as much as 0.5 km of fault-normal offset of the computed hypocenters to the southwest, but much less along-strike where velocity gradients are smaller (Michelini and McEvilly, 1991; Eberhart-Phillips and Michael, 1993). Depth bias is unknown, but we expect it to be small, constrained by *P* and *S* observations at epicentral distances less than the focal depths and by well-determined shallow velocities (Vibroseis measurements and calibration explosions).

Temporal Organization within Clusters

The eight distinct characteristic event sequences in the Kester group exhibit fairly stable recurrence intervals through the observation period, as illustrated in the upper panel of Figure 8. Our data provide only a minimal demonstration of regularity since events are surely missed during normal network outages, because of imperfect triggering (detection is required at three stations), or during Vibroseis monitoring sessions when the network is not operating in the microearthquake mode. Yet, even with this incomplete detection, the intrinsic uncertainty in the observed recurrence intervals is 0.35 for these Parkfield sequences (0.0 describes exact time predictability; 1.0 represents an unpredictable Poisson process; see, e.g., Dieterich, 1990). This value is comparable to that of large repeating earthquakes globally. A prediction exercise is underway for a different group of 13 cluster sequences at Parkfield (including K7 from this study) that collectively exhibit intrinsic uncertainty of 0.21 (Nadeau, 1996).

Because of detectability limits, the regularity of repeating sequences at $Mw < 0.9$ is generally not revealed in the NCSN catalog C1, as shown in the lower panel of Figure 8. There may also be sequences with greater recurrence intervals as yet not identified in the HRSN data. Our comprehensive and computationally intensive, cross-correlation search of waveforms for the 4000+ events has extended only through 1992, so that identification of recurrence intervals greater than about three years is incomplete. Also, the limited dynamic range of our monitoring network results in badly clipped signals for $Mw > 2.0$, confounding similar-event identification by cross-correlation of windowed *P* and *S* arrivals, although we may be able to identify some of them through their highly repeatable unclipped coda waveforms

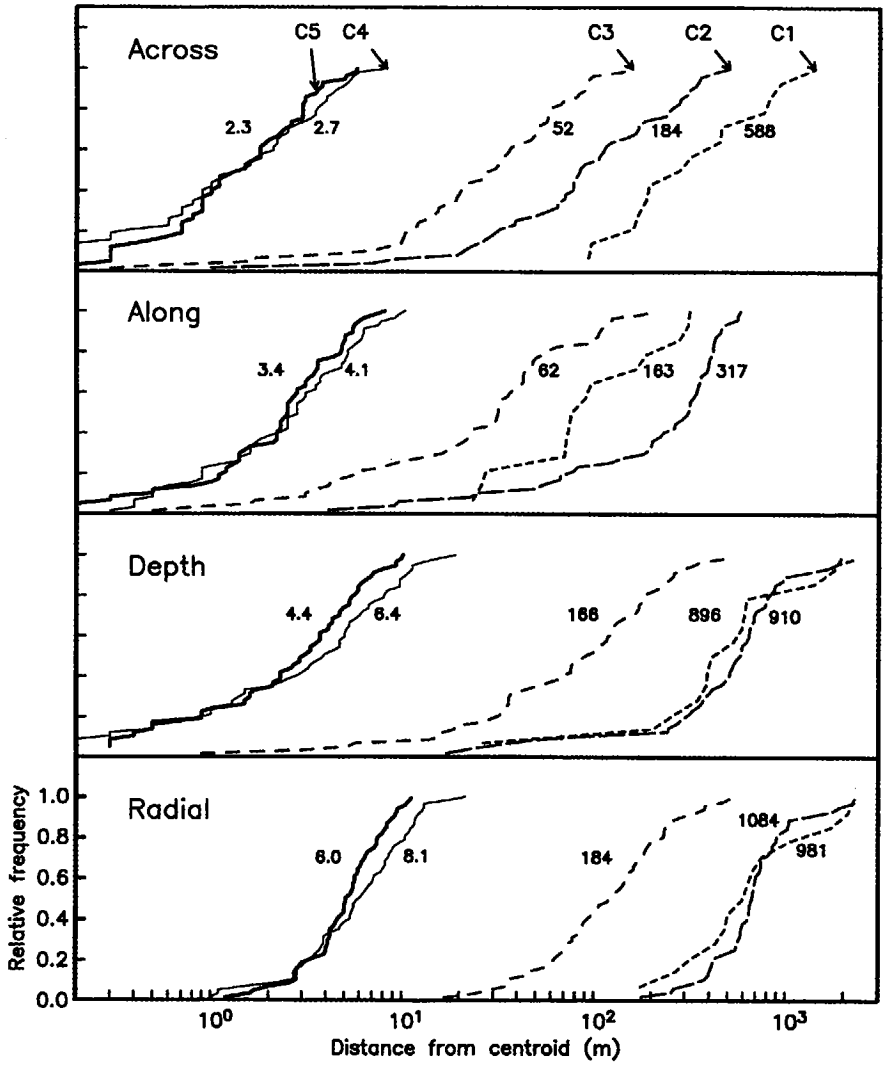

Figure 7. Comparing catalog resolutions. Distributions of distances from characteristic event centroids in three fault-referenced directions and radially for the characteristic events in the five catalogs. Numbers are standard deviations of the distances in meters. The distributions measure catalog resolution under the assumption of colocated events within the characteristic sequences. Note the log scale used for the event-to-centroid separation distances. The five catalogs differ in resolution by more than two orders of magnitude, and it appears that high-quality data processed using subsample relative timing among highly similar waveforms can yield relative hypocenter location accuracy of about 5 m.

and by using complementary NCSN recordings at greater distances. Repeating sequences of events larger than $Mw = 2$ may not have been recognized solely by spatial proximity in the NCSN catalog because of the location errors illustrated in Figures 4 and 7. Other investigations, based on NCSN-type data, have reported repeating clustered events for small- to intermediate-sized events on the San Andreas fault system (e.g., McNally, 1976; Ellsworth and Dietz, 1990; Vidale *et al.*, 1994; Beroza *et al.*, 1995), but the bandwidth limits and location uncertainties previously discussed probably result in some incomplete and ill-defined sequences, particularly below the M 2 to 3 level.

Average recurrence times for the repeating sequences in the Kester group range from a few months to about 2 years and scale with event magnitude as shown in Figure 9. It is possible that a continuum of characteristic event sequences exists through the magnitude range up to the sequence of past M 6 earthquakes at Parkfield. Simple linear extrapolation of the relationship in Figure 9 yields the interesting results of a zero recurrence interval somewhere below $Mw = -0.5$ (roughly the lower limit of the network detection capability) and a recurrence interval of about 10 years for $Mw = 6$. If, however, the data in Figure 9 are fit with a

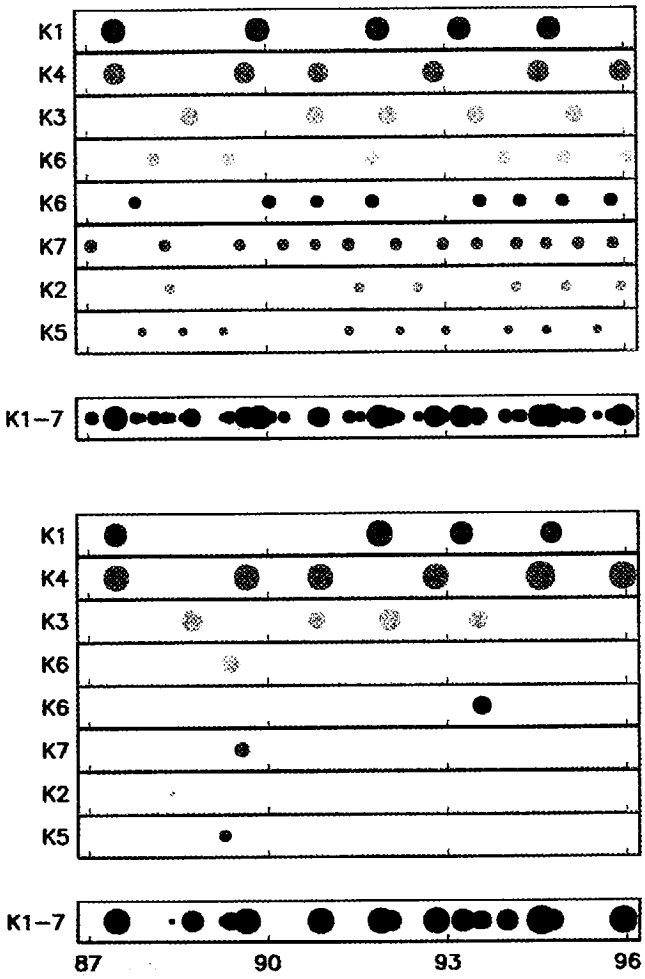

Figure 8. Recurrence patterns within clusters. *Upper panel:* Occurrence times for the eight characteristic sequences (K6 contains two) from the Parkfield HRSN catalog plus one event in K1 (day 321 of 1991) missed because of the Vibroseis experiment. Symbol size is proportional to magnitude in the range 0.2 to 1.3. Time-line K1 to K7 of all Kester group events illustrates the difficulty in identifying the individual sequences without benefit of high-resolution data. Undetected events in the sequences make this a display of minimal regularity. *Lower panel:* The same presentation of occurrence times for the Kester events contained in the NCSN catalog (coda magnitudes 0.0 to 1.5). Incomplete detection of events with $Mw < 0.9$ becomes increasingly severe so that process regularity on the scale of months within the fault zone cannot be accurately estimated.

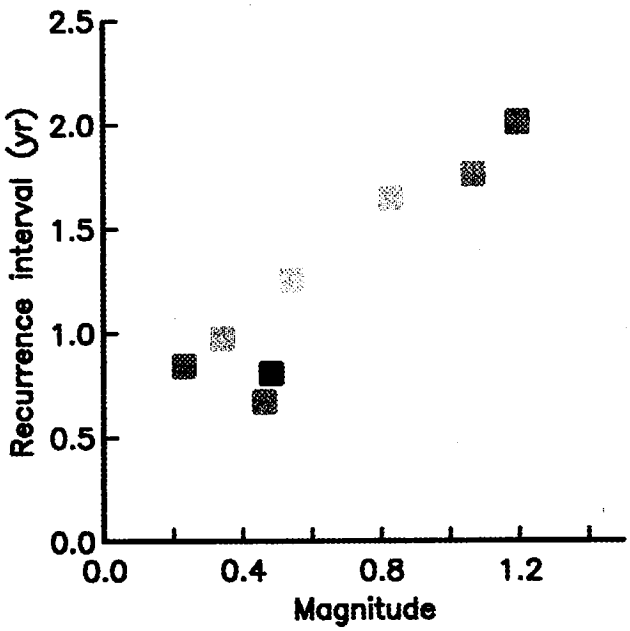

Figure 9. Recurrence times versus magnitude. Median recurrence intervals (to minimize the effect of missed events) scale with clustered event magnitudes showing that in a fault-zone drilling program, waiting times for events within the Kester group could be as short as a few months (and this figure includes only about one-third the seismicity in the local zone).

constant stress drop model (Nadeau, 1995), the predicted M 6 recurrence interval is about 500 years.

The recurrence-magnitude relationship for the small events in this study has implication for scaling of their stress drops. Assuming a constant tectonic loading rate that produces repeated slip on the same circular surface, recurrence time will be proportional to the product of static stress drop and rupture radius so that for fixed patch size stress drop must increase with magnitude. Alternatively, for a constant stress drop with magnitude, our apparent fixed patch size cannot represent the full slip surface for all clusters. Slip surfaces may extend beyond these patches into the aseismic intercluster space that makes up about 98% of the fault surface. There is some evidence for cluster interaction to a range 100 m or more (Nadeau *et al.*, 1994, 1995; Johnson and McEvilly, 1995); however, the observation that adjacent but nonoverlapping subclusters exhibit unique recurrence patterns argues against overlapping slip surfaces, suggesting that seismic slip is confined to the localized cluster patch and does not extend into adjacent areas. Equally possible is magnitude-dependent patch size and constant stress drop in a situation where our resolution cannot detect variations in source dimensions below about a 5-m radius. Consequences of this otherwise attractive possibility are unconventionally high stress drops for these small repeating sources. For example, confining the $Mw = 1.3$ events to the 5-m patch implies a constant stress drop of about 400 MPa. Subsequent work by Nadeau and Johnson (1997) has investigated repeating clustered sequences, extending the magnitude range to the M 6 Parkfield sequence, and finds strong dependence of stress drop on magnitude.

Drilling to a Shallow Hypocenter?

Having developed this detailed picture of microearthquake activity at Parkfield, we progressed naturally to con-

sidering implications for *in situ* measurement of the process. Primary goals of a fault-zone drilling program are to penetrate and sample the fault at a depth where earthquakes occur and, second, if possible, to drill through a site of expected earthquake slip in order to monitor nucleation, rupture, and postseismic phenomena (hydrologic, chemical, thermal, lithologic, etc.). The planar surface defined by the microearthquakes at the Kester site presumably delineates the actively slipping San Andreas fault and thus presents a target, if reached, that would achieve both goals. The precise relative locations and regular occurrence of the Kester events suggest a strategy for deep drilling into the fault zone, penetrating the focus of a future microearthquake. The target would be a small vertical disk in the fault plane where a repeating event of known magnitude is anticipated (Fig. 8). Selecting a magnitude defines the likely waiting time for its occurrence (Fig. 9), a factor of significance when instrumenting the hostile environment of an active fault zone.

The microearthquakes in the target group beneath the proposed drilling site at Parkfield occupy a vertical strip about 1 km wide (along-fault dimension) parallel to the active San Andreas fault trace. On average, there is an event somewhere on this surface every 2 months (or every few weeks if we consider the rest of the seismicity in the immediate vicinity of the eight sequences considered here). The four clusters at the upper edge of this strip lie about 3 km below the surface, within practical drilling range,and produce an event about every 3 months (perhaps 1 to 2 months considering all the seismicity). It is thus possible to select the occurrence time and magnitude of a targeted earthquake in this zone with a precision and confidence useful to a drilling and instrumentation experiment.

The unknown location bias remains a serious impediment to implementation of a targeted drilling experiment. While the relative locations of events in the constellation of potential targets are precisely known, the strong lateral velocity gradients across the fault zone introduce a fault-normal hypocenter bias of as much as 0.5 km to the southwest of the fault zone. Obviously, this bias must be determined and removed. In the drilling process, measurements in the borehole, temporary surface arrays, and drill-bit imaging technology (e.g., Rector and Weiss, 1989) can be used to calibrate progressively the acoustically determined drill-bit position to an accuracy of 5 to 25 m (J. W. Rector, personal comm., 1997) and thus the hypocenters of events that occur during the drilling operation (an event every 2 months in the Kester group). Inspection of HRSN waveforms will assign any event to its proper cluster, and the entire constellation of clusters gets repositioned, converging during the drilling and monitoring phase to the absolute locations needed to select the target for fault-zone penetration. That selection would be based on the known recurrence history for the constellation (Fig. 8), allowing sufficient time for instrument emplacement.

The drilling will likely perturb the nucleation process if the microearthquake source volume is penetrated late in the repeat cycle. In practice, it will be prudent to drill to within a few source dimensions of the impending slip, emplace the monitoring instrumentation, and penetrate the slip surface immediately after the microearthquake occurrence.

This hypothetical experiment has the attractive feature of targeting a specific earthquake, selecting both its magnitude and occurrence time. The general goal of intersecting a seismogenic fault zone and sampling its environment can be achieved at many different locations in the world, but scientific prospects are enhanced substantially by the promise of being able to have a monitoring system installed within an earthquake source volume at the time of rupture. Such an exercise is only possible where comparable resolution of meters for hypocenters is attainable and where a characteristic behavior in microearthquakes has been established. Parkfield today may well be unique in these attributes.

Acknowledgments

The Parkfield High-Resolution Seismographic Network functions through close cooperation among researchers at the University of California at Berkeley, the U.S. Geological Survey, and the Lawrence Berkeley National Laboratory (LBNL). The USGS provides primary financial support through NEHRP Award 1434-95-G2540. Data processing is done at the Center for Computational Seismology (CCS) at LBNL, which is operated by the University of California for the U.S. Department of Energy under Contract No. DE-AC03-76SF00098, and CCS is supported by the DOE Office of Basic Energy Sciences. Partial postdoctoral salary support (RN) came from Lawrence Livermore National Laboratory through an IGPP grant.

References

Aster, R. C. and J. Scott (1993). Comprehensive identification of similar earthquakes in microearthquake data sets, *Bull. Seism. Soc. Am.* **83,** 1307–1314.

Bakun, W. H. and A. G. Lindh (1985). The Parkfield, California, prediction experiment, *Earthquake Predict. Res.* **3,** 285–304.

Bakun, W. H. and T. V. McEvilly (1984). Recurrence models and Parkfield, California earthquakes, *J. Geophys. Res.* **89,** 3051–3058.

Beroza, G. C., A. Cole, and W. Ellsworth (1995). Stability of coda wave attenuation during the Loma Prieta, California, earthquake sequence, *J. Geophys. Res.* **100,** 3977–3987.

Dieterich, J. H., Chairman, Working Group on California Earthquake Probabilities (1990). Probabilities of large earthquakes in the San Francisco bay region, California, *U.S. Geol. Surv. Circ. 1053,* 51 p.

Eberhart-Phillips, D. and A. J. Michael (1993). Three-dimensional velocity structure, seismicity, and fault structure in the Parkfield region, central California, *J. Geophys. Res.* **98,** 1153–1172.

Ellsworth, W. L. (1996). Drilling into the earthquake source: the search for a site to test theories of earthquake generation at Parkfield, *Ext. Abstract VIII International Symposium on Observation of the Continental Crust through Drilling,* Tsukuba, Japan.

Ellsworth, W. L. and L. D. Dietz (1990). Repeating earthquakes: characteristics and implications, *Proc. of Workshop XLVI,* the 7th U.S.–Japan Seminar on Earthquake Prediction, U.S. Geol. Surv. Open-File Rept. 90–98, 226–245.

Fremont, M.-J. and S. D. Malone (1987). High precision relative locations of earthquakes at Mount St. Helens, Washington, *J. Geophys. Res.* **92,** 10223–10236.

Hickman, S., M. Zoback, L. Younker, and W. Ellsworth (1994). Deep scientific drilling in the San Andreas fault zone, *EOS* **75,** 137.

Johnson, P. A. and T. V. McEvilly, (1995). Seismicity at Parkfield and the

possible involvement of fault-zone fluids, *J. Geophys. Res.* **100,** 12937–12950.

Karageorgi, E., R. Clymer, and T. V. McEvilly (1992). Seismological studies at Parkfield. II. Search for temporal variations in wave propagation using Vibroseis, *Bull. Seism. Soc. Am.* **82,** 1388–1415.

Michelini, A. and T. V. McEvilly (1991). Seismological studies at Parkfield: I. Simultaneous inversion for velocity structure and hypocenters using B-splines parameterization, *Bull. Seism. Soc. Am.* **81,** 524–552.

McNally, K. C. (1976). Spatial, temporal, and mechanistic character in earthquake occurrence: a segment of the San Andreas Fault in central California, *Ph.D. Thesis,* University of California, Berkeley, 172 pp.

Nadeau, R. M. (1995). Characterization and application of microearthquake clusters to problems of scaling, fault zone dynamics, and seismic monitoring at Parkfield, California, *Ph.D. Thesis,* University of California, Berkeley, 200 pp.

Nadeau, R. M. (1996). Recurrence scaling of characteristic microearthquakes at Parkfield with large repeating events on the San Andreas fault in California, *Seism. Res. Lett.* **67,** 48.

Nadeau, R. M. and L. R. Johnson (1997). Seismological studies at Parkfield VI: moment release rates and estimates of source parameters for small repeating earthquakes, *Bull. Seism. Soc. Am.,* submitted.

Nadeau, R. M., M. Antolik, P. Johnson, W. Foxall, and T. V. McEvilly (1994). Seismological studies at Parkfield III: microcarthquake clusters in the study of fault-zone dynamics, *Bull. Seism. Soc. Am.* **84,** 247–263.

Nadeau, R. M., W. Foxall, and T. V. McEvilly (1995). Clustering and periodic recurrence of microearthquakes on the San Andreas fault at Parkfield California, *Science* **267,** 503–507.

Poupinet, G., W. L. Ellsworth, and J. Frechet (1984). Monitoring velocity variations in the crust using earthquake doublets: an application to the Calaveras fault, California, *J. Geophys. Res.* **89,** 5719–5731.

Rector, J. W. and D. S. Weiss (1989). Real-time drill bit VSP from an offshore platform, *59th Annual Int. Mtg., Soc. Expl. Geophys. Expanded Abstracts* **89,** 5–7.

Schwartz, D. P. and K. J. Coppersmith (1984). Fault behavior and characteristic earthquakes: examples from the Wasatch and San Andreas faults, *J. Geophys. Res.* **89,** 5681–5698.

Vidale, J., W. Ellsworth, A. Cole, and C. Marone (1994). Variations in rupture process with recurrence interval in a repeated small earthquake, *Nature* **368,** 624–626.

Earth Sciences Division, MS 90-1116
Lawrence Berkeley National Laboratory and Seismological Laboratory
University of California
Berkeley, California 94720

Manuscript received 20 February 1997.